Electro-entropic excluded volume effects on DNA looping and relaxation in nanochannels

Yeng-Long Chen[1,2,3,a)]
[1]Institute of Physics, Academia Sinica, Taipei, Taiwan
[2]Department of Chemical Engineering, National Tsing-Hua University, Hsinchu, Taiwan
[3]Department of Physics, National Taiwan University, Taipei, Taiwan

(Received 1 October 2013; accepted 7 October 2013; published online 22 October 2013)

We investigate the fluctuation-relaxation dynamics of entropically restricted DNA molecules in square nanochannels ranging from 0.09 to 19.9 times the persistence length. In nanochannels smaller than the persistence length, the chain relaxation time is found to have cubic dependence on the channel size. It is found that the effective polymer width significantly alter the chain conformation and relaxation time in strong confinement. For thinner chains, looped chain configurations are found in channels with height comparable to the persistence length, with very slow relaxation compared to un-looped chains. Larger effective chain widths inhibit the formation of hairpin loops. [http://dx.doi.org/10.1063/1.4826157]

INTRODUCTION

Stiff biological macromolecules such as actin filaments and DNA are restricted in partitions comparable to or much smaller than their longest characteristic length, inside a natural environment such as the cell and a cell nucleus. The strong confinement constraint rearranges the structure of the molecules and also affects the dynamics of processes such as nucleosome folding/unfolding, DNA transcription, and actin polymerization. Advances in nano-fabrication have greatly facilitated studies that directly probe changes to a single polymer structure and dynamics in confinement[1–18] in well-defined nanoslits and nanochannels. These studies typically adopt double stranded viral phage DNA molecules as model polymers due to its mono-dispersity, long persistence length ($P \approx 50$ nm at high ionic strength), and the ease of direct observation. Several recent studies have examined the conformation and relaxation of a semi-flexible chain (SFC) in sub-persistence length quasi-one dimensional (Q1D) square nanochannels and found that these properties are qualitatively different from unconfined SFC.[5,19–23] Due to the strong restriction on coordinated segmental motion in nanochannels, the dominant segmental motions are not yet clear. In this study, measurements of DNA extension and dynamics are compared to predictions for chains in sub-persistence nanochannels and the results from Brownian dynamics simulations (BDs). We investigated how changes in the effective polymer width and the bulk persistence length, which may be controlled by varying solvent ionic strength,[24,25] affect the confined polymer properties. The chain relaxation mechanisms are found to depend on both the strong confinement and the effective polymer width.

The physical properties of a SFC can be considered on the length scales of the monomer width σ_m, the persistence length P, the radius of gyration in free solution $R_{g,bulk}$, and the contour length $L = (N-1)\sigma_m$, where N is the number of monomers. Depending on which length scale one probes a polymer, it can exhibit both flexible rod-like ($<P$) and coil-like ($>R_{g,bulk}$) characteristics. For double stranded λ-phage DNA, $P = 50$ nm and $L = 16\,\mu$m are separated by

a)Electronic mail: yenglong@phys.sinica.edu.tw

nearly three orders of magnitude. Confinement effects begin to significantly restrict accessible polymer conformations when the channel height H is comparable to $R_{g,bulk}$.

A scaling argument can provide some insight to how the chain relaxation time depends on confinement for $R_g > H > P$. Scaling theory[26–28] predicts that the chain size in a channel would increase $\sim H^{-2/3}$ for self-avoiding chains (SAW) and $\sim H^{-1}$ for Gaussian chains (GCs). In small $(H < P)$ channels, the chain extension X is the projection of (L/l) deflection segments stretched along the channel length, with the deflection length $l = (H^2P)^{1/3}$.[19] For a small deflection angle $(H/l \ll 1)$, $X = L[1 - A(H/P)^{2/3}]$, with the predicted value of $A = 0.17$ verified in recent MC studies.[5,17,29,30]

For unconfined polymers, the longest relaxation time is $\tau_{bulk} = (R_g{}^2/D)$, where $D = \langle(\boldsymbol{R}(t)\text{-}\boldsymbol{R}(0))^2\rangle/(6\,t)$ is the chain diffusivity and $\boldsymbol{R}(t)$ is the chain center-of-mass position at time t. In Q1D confinement, the longest chain relaxation time is the reptation time $\tau_{Q1D} \sim R_g{}^2/D \sim [N(P/H)^{-2/3}]^2/D \sim N^3$. In free solution, if intra-chain hydrodynamic interactions (HIs) were neglected, the bulk solution diffusivity $D \sim N^{-1}$ and $\tau_{bulk} \sim NR_g{}^2 \sim N^{11/5}$ (SAW) and $\sim N^2$ (GC).[31] Thus, a scaling law $\tau/\tau_{bulk} \sim (R_{g,bulk}/H)^{\nu}$ with the exponents $\nu = 4/3$ (SAW) and 2 (GC) are found for the intermediate region. With intra-chain HI, $D \sim R_g{}^{-1}$, $\tau_{bulk} \sim N^{9/5}$ (SAW), and $N^{3/2}$ (GC) for free polymers.[31] Following the same argument, the scaling exponents are $\nu = 2$ (SAW) and 3 (GC) for the intermediate region. The qualitative dependence is consistent with the idea that chain relaxation slows as the chain becomes more confined. It is also expected that τ depends more strongly on H for the Gaussian chain due to the greater change in the chain fractal dimension.

However, a recent experiment showed that the chain stretch relaxation time has a non-monotonic dependence on the channel height.[5] In nanochannels, the conformational restriction results in a large separation between the chain and segmental relaxation times. The dominant segmental relaxation process thus depends on the transverse correlation length, with $\tau \sim l_\perp{}^2/D_{seg} \sim H^2/D_{seg}$, where D_{seg}, is the segment diffusivity. For the channel-deflected segments, one may consider the segments of length H to be rod-like, with the segmental diffusivity $D_{seg} \sim \ln(H/\sigma_m)/H$ and $\tau \sim H^3/\ln(H/\sigma_m)$.[31]

METHOD

To examine the fluctuation-relaxation process of chain segments in the nanochannel, Brownian dynamics simulations with and without HIs are employed to track the chain trajectory,[32–37]

$$-\zeta[v_p - v_f(\boldsymbol{r}_i)] + \boldsymbol{f}_i^R(t) - \frac{\partial U}{\partial \boldsymbol{r}_i} = 0. \tag{1}$$

The friction force is determined from the friction coefficient of a bead ζ, the monomer bead velocity v_p, and the fluid velocity $v_p(\boldsymbol{r}_i)$. $\boldsymbol{f}_i^R(t)$ is a random force that satisfies the fluctuation-dissipation theorem, with a Gaussian distribution with zero mean and a variance $2k_BT\zeta/dt$. Intra-chain hydrodynamic interaction is determined by coupling the polymer to a lattice Boltzmann fluid with thermal fluctuations, where the friction forces acting on the polymer are exchanged to the fluid with full coupling.[33] The bead-wall repulsive interaction is a cubic potential with a range of σ_m.[38] The integration time step is $dt = 5 \times 10^{-3}\,\tau_D$, where $\tau_D = \zeta\sigma_m{}^2/k_BT$ is the bead diffusion time. With the viscosity with of water at 298 K, $dt = 0.091$ ns for $\sigma_m = 2$ nm.

In order to capture how strong confinement affects the chain rigidity in a Q1D channel, two coarse-grained double stranded DNA molecules with 40 and 160 persistence lengths are examined. The total chain lengths are $N = 160$, 400, 800, and 1000 beads. Hydrodynamic interactions is included only for $N = 160$ due to the significant computation cost. Each spring has equilibrium length σ_m, which is the chosen unit length. The spring potential energy is

$$U_{spring} = \frac{k_v k_B T}{2\sigma_m^2} \sum_i (|\boldsymbol{r}_i - \boldsymbol{r}_{i+1}| - \sigma_m)^2, \tag{2}$$

where $k_v = 400$ for a harmonic spring is chosen to capture the rigidity of the double helix, and $k_BT = 1$. $\boldsymbol{r}_i$ is the position of the i-th bead. The beads repel each other with a short range

repulsive Morse potential with a cutoff distance of 1.5 to coarsely mimic the inter-segmental steric and electrostatic repulsion,

$$U_{M,rep} = \varepsilon_m k_B T \sum_{i,j} \exp[-\alpha_m (r_{i,j} - \sigma_m)], \tag{3}$$

with $\varepsilon_m = 0.2$, $\alpha_m = 6$, such that the monomer core radius is $0.5\sigma_m$. $r_{i,j}$ is the distance between the i-th and j-th beads. The chain rigidity is defined by a bending potential of the angle between $\boldsymbol{v}_{i-1} = (\boldsymbol{r}_{i-1}\text{-}\boldsymbol{r}_i)$ and $\boldsymbol{v}_i = (\boldsymbol{r}_i\text{-}\boldsymbol{r}_{i+1})$,

$$U_{bend} = k_{bend} k_B T \sum_i \left(1 - \frac{\boldsymbol{v}_{i-1} \cdot \boldsymbol{v}_i}{|\boldsymbol{v}_{i-1}||\boldsymbol{v}_i|}\right). \tag{4}$$

The persistence length is determined from the exponential decay of the segmental correlation function $C(j) = \langle \boldsymbol{v}_i \cdot \boldsymbol{v}_{i+j} \rangle$. k_{bend} are chosen such that $P/\sigma_m = 4$, 5, 10, and 25 for $N = 160$, 800, 400, and 1000, respectively. By matching P to the measured DNA persistence length, the effect of increasing effective chain widths in a channel of length $2000 \times H \times H$ is observed.

DNA persistence length increases as the solution ionic strength decreases due to stronger electrostatic repulsion. The model bead excluded volume diameters correspond to the change of polymer width due to the electrostatic screening length (high ionic strength). $P/\sigma_m = 25$ corresponds to the bare DNA with $\sigma_m = 2.0$ nm. Based on prior studies, the model chain with $P/\sigma_m = 4$, 5, and 10 are matched to effective DNA widths of $\sigma_m = 16.6$, 12.2, and 5.1 nm in 0.006, 0.016, and 0.12 M monovalent salt solutions.[24,25]

RESULTS AND DISCUSSION

The chain conformation is analyzed from the chain extension, $X = \max(x_i) - \min(x_i)$, as illustrated in Fig. 1(a). Ensemble properties are calculated from more than 100 trials of chain relaxation trajectories, each trial length is at least 5 chain relaxation times. In free solution, $R_{g,bulk}/P = 3.65 \pm 0.18$, 2.96 ± 0.09, 6.58 ± 0.22, and 3.46 ± 0.12 for $N = 160$, 400, 800, and 1000, respectively. The extensional relaxation of initially nearly fully stretched chains is captured as each chain relaxes via an individual trajectory. The equilibrium chain stretch $\langle X \rangle$ is shown in Fig. 1(a). As observed in prior studies,[5,14,17,39] there are multiple regimes of conformation change. for $H < R_{g,bulk}$, $\langle X \rangle$ increases following $H^{-2/3}$ as expected for SAW. As H approaches P, it is found that $\langle X \rangle$ deviates from the expected scaling, possibly due to the

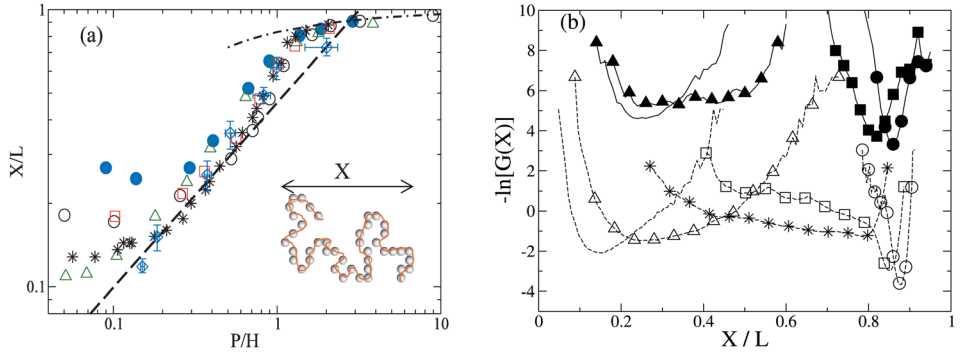

FIG. 1. (a) Equilibrium chain stretch as a function of P/H for $N = 160$, $P/\sigma_m = 4$ (filled circle), $N = 1000$, $P/\sigma_m = 25$ (circle), $N = 400$, $P/\sigma_m = 10$ (square), $N = 800$, $P/\sigma_m = 5$ (triangle). Data from Refs. 17 (star) and 5 (diamond with error bars) are also shown. Scaling predictions of $(P/H)^{2/3}$ (dashed line), (P/H) (solid line) and Eq. (1) (dotted-dashed line) are also shown. Inset: Illustration of the chain dimension. (b) The configuration free energy for $N = 160$, $P/\sigma_m = 4$ (solid lines) in nanochannels with $H/P = 14.5$, 3.2 (triangle), 0.95 (square), and 0.7 (circle) and $N = 1000$, $P/\sigma_m = 25$ chains (dashed lines) in nanochannels of $H/P = 9.9$, 1.9 (triangle), 1.1 (star), 0.9 (square), 0.3 (circle). The data for $N = 160$ are shifted up by 2 for clarity.

depletion of intra-chain loops.[23,40] For $H < P$, Eq. (1) captures the chain extension dependence with $A = 0.17$.

For chains with the same number of persistence lengths ($N = 160$, 400, and 1000), $\langle X \rangle$ increases as the effective chain width increases due to the increased equilibrium chain stretch, but the qualitative dependence for $H < R_g$ does not change. The results for $N = 1000$, $P/\sigma_m = 25$ agrees very well with MC results[17] for $H < R_g$, and also with the experimental results[5] except for the smallest nanochannel.

Deviation of $\langle X \rangle$ from the scaling law prediction for $H \approx P$ nanochannels is investigated by examining the chain configuration free energy -ln($G(X)$), with the chain stretch distribution function $G(X)$, as shown in Fig. 1(b). The configuration free energy of $N = 1000$, $P/\sigma_m = 25$ exhibits a sharp minimum for $H/P = 9.9$. As H decreases, the free energy minimum broadens and the curvature flattens as H decreases to $0.9P$, which indicates the presence of hairpin configurations with the chain looping on itself in the nanochannel as reported in MC simulations.[17,22,39,41] For smaller H, the minimum shifts to higher X and finally become a single minimum. The coexistence of looped and extended configurations for $H \approx P$ is analogous to an intermediate state during the transition from coil to stretch configurations under an external extensional force.

The broad distribution for X is not found for $P/\sigma_m = 4$ and 5, which reflects the packing constraints of chain segments inside small channels and the inhibition of chain folding for the larger effective width. This would correspond to stronger electrostatic repulsion between DNA segments and between the segments and the walls at lower ionic strength. The reduction of chain folding at low ionic strength could explain observations of higher-than-expected average DNA extension in low-salt solution in nanoslits[6,42] and nanochannels.[43]

BD allows direct probing of the relationship between chain conformation and relaxation from individual chain relaxation trajectories, as illustrated in Fig. 2. For $P/\sigma_m = 25$ and $H/P = 9.9$, the chains relax to a small equilibrium extension ($\langle X/L \rangle = 0.17 \pm 0.01$, Fig. 2(a)) following a single fast exponential decay. For $H \ll P$, the chains become highly extended with hairpin loops inhibited, and the chain relaxation follow a single exponential decay. However, for $H/P \approx 1$, very different relaxation trajectories are found. Fig. 2(a) shows two fast relaxation trajectories to an extended conformation, with $\langle X/L \rangle = 0.63 \pm 0.03$. Other trajectories are

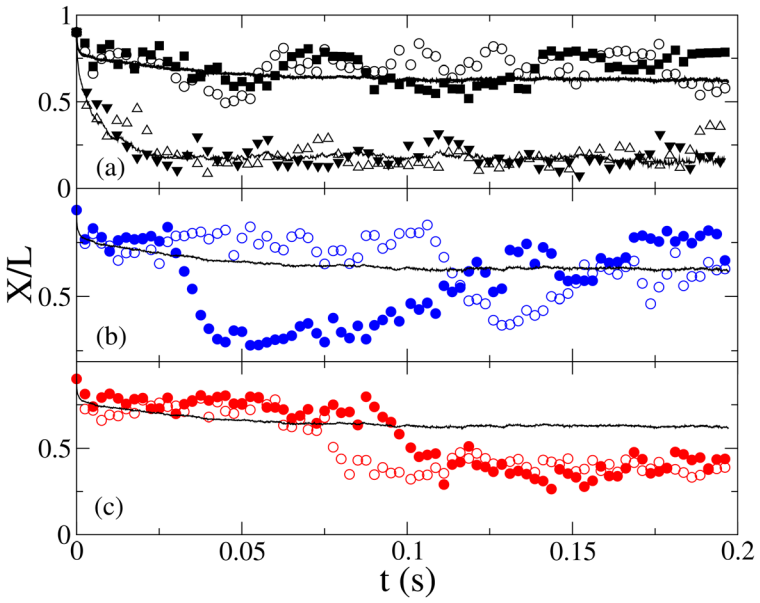

FIG. 2. Selected chain stretch relaxation trajectories (circles) and $\langle X(t) \rangle$ (solid line) showing non-looped (a), relaxed loops (b), and un-relaxed loops (c) for $N = 1000$, $P/\sigma_m = 25$, $H/P = 1$. Trajectories in channels with $H/P = 9.9$ (triangles) are shown in (a).

observed to relax slowly to reduced chain extension conformations due to folding with long lifetimes. The relaxation times of the folded states vary, as some looped states become unfolded (Fig. 2(b)), while other trajectories enter and remain in the looped state for extended period (Fig. 2(c)). The ensemble average of 100 trajectories shows both the fast ($t < 0.01$ s) and the slow relaxation processes.

The chain relaxation time (τ_{relax}) can be directly measured from the stretch-relaxation process and the fluctuation correlation function in $H < P$ nanochannels. For $R_g > H > P$ channels, chain stretch relaxation exhibits exponential decay as expected, as shown in Fig. 3(a) inset.[31,44] Fig. 3(a) shows the stretch relaxation function $R_X(t) = (X(t) - \langle X \rangle)^2 \sim \exp(-2t/\tau_X)$ with the relaxation time τ_X.[45,46] With stronger spatial restrictions in the nanochannel, coordinated segmental relaxation processes such as whole chain reorientation become more inhibited. For $H \approx P$, fast and slow relaxation regimes are both observed. They correspond to the fast contraction of the chain from the initial stretched configuration to when the segments encounter the channel walls, and the slower relaxation of wall-confined segments. Prior studies of DNA in nanoslits have also found a separation of segmental relaxation and coordinated chain rotation times.[1] In Q1D nanochannels, coordinated chain rotation is strongly inhibited, leading to a large separation between segmental relaxation and chain reptation. For comparison to experiments,[5] which measured the fluctuation correlation time from the fluctuation correlation $C_\delta(t) = \langle \delta X(0) \delta X(t) \rangle \sim \exp(-t/\tau_\delta)$, $\delta X(t) = X(t) - \langle X \rangle$, as shown in Fig. 3(b). τ_δ is found to agree well with slow stretch relaxation time τ_X.

Accounting for HI significant quickens chain relaxation time for $R_g > H > P$, as observed for $P/\sigma_m = 4$ in Fig. 4 inset. With HI, stronger dependence on H is observed. Without accounting for HI, τ does not change significantly for $P/\sigma_m = 4$ and 5 as H decreases for $R_g > H > P$, in contrast to the expected $H^{-3/4}$ dependence, due to the limited range between R_g and P. For $P/\sigma_m = 10$ and 25, τ increases and reaches a maximum near $H/P = 1$. The delayed transition and longer relaxation time near $H \approx P$ for $P/\sigma_m = 25$ may be attributed to the slow relaxation of loops.

For $H < P$, τ is found to decrease sharply as H decreases, with and without HI. The transition occurs near $H = P$ except for $P/\sigma_m = 25$, which may be due to slower loop relaxation for the thinner chain. For $P/\sigma_m = 25$, the transition at $H \approx 0.6P$ corresponds to the disappearance of the long tail in $G(X)$ at which height the chain cannot fold by looping due to strong segmental repulsion. For $P/\sigma_m = 4$ and 5, chain folding is inhibited by the large effective chain width at channel height $H \approx P$. For all chains, τ consistently decrease as $H^3/\ln(H/\sigma_m)$ if slower loop relaxation is eliminated.

The observed strong dependence on the effective chain width indicates that segmental motions could be strongly influenced by the electrostatic repulsion and the solution ionic strength, corresponding to the lack of chain folding for effectively wider chains in nanochannels. Interestingly, we note that even with the very coarse-grained polymer model for the DNA

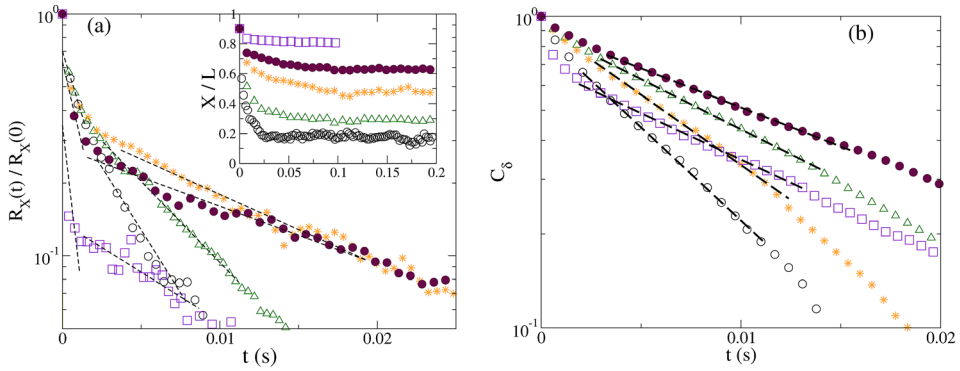

FIG. 3. (a) The stretch relaxation function $R_X(t)$ for $N = 1000$, $P/\sigma_m = 25$, for $H/P = 9.9$ (circle), 1.9 (triangle). 1 (star), 0.9 (filled circle), 0.6 (square). The dashed lines indicate the exponential fits to extract the relaxation time. Inset: The relative chain stretch $X(t)/L$. (b)The fluctuation correlation function $C_\delta(t)$ for the same H/P as in (a).

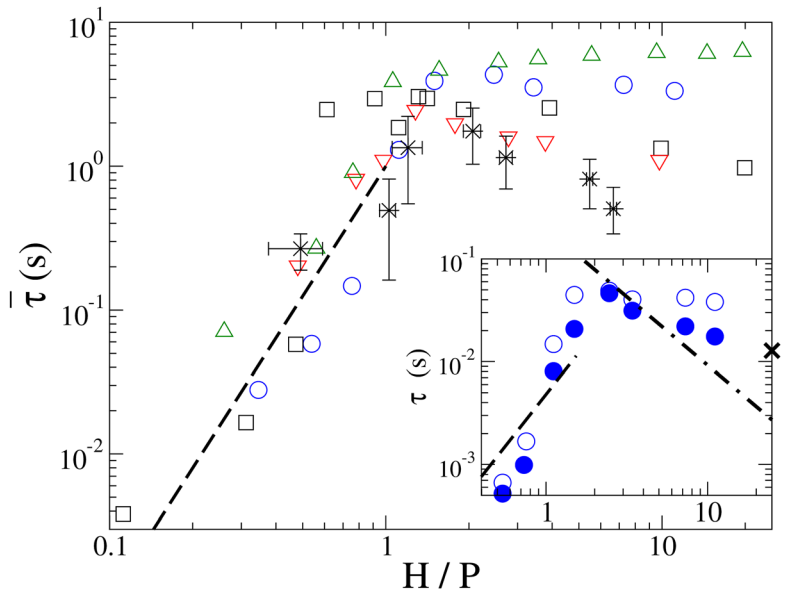

FIG. 4. The scaled chain relaxation time for $N = 1000$, $P/\sigma_m = 25$ (circles), $N = 400$, $P/\sigma_m = 10$ (squares), and $N = 800$, $P/\sigma_m = 5$ (triangles). Data from Ref. 5 are shown as stars with error bars. Chain relaxation time is rescaled according to its dependence on the chain contour length, $\bar{\tau} = \tau_\delta (L_\lambda/L)^{11/5}$, $L_\lambda = \lambda$-DNA contour length of 16 μm. The inset shows the relaxation time with (filled circle) and without HI (empty circle) for $N = 160$, $P/\sigma_m = 4$. **X** marks the estimated τ_{bulk} for $L = 2$ μm. The dashed and dotted-dashed lines show $H^3/\ln(H/\sigma_m)$ and $(H/P)^2$ dependences, respectively. The error estimates are comparable to the symbol size.

molecule, the rescaled relaxation time is in reasonable agreement to the experimental data within the error bars.

CONCLUSIONS

In this study, we found that Brownian dynamics simulations of chain properties with a coarse-grained DNA model capture the inhibition of long wave length segmental relaxation in strong confinement, and predictions of the chain relaxation time are in good agreement with a prior experiment. It is also found that the effective DNA width can determine whether DNA can fold inside a nanochannel comparable to its persistence length, and intra-chain repulsive interactions can strongly affect polymer dynamics for polymers under strong confinement. Our study finds that the chain dynamics have qualitatively different behavior depending on whether the molecule is able to form loops in the nanochannel, which suggests that experimental ionic strength for DNA molecules in nanochannels needs to be carefully controlled. Furthermore, reaction mechanisms that depend on loop formation, such as proteins that require two binding sites far apart on the chain backbone, would be strongly affected by the strong confinement and ionic conditions.

Editorial Note: This paper, along with Ref. 47, is part of a coordinated submission of two contributions with different approaches to the same phenomenon.

ACKNOWLEDGMENTS

Funding for this study comes from the Academia Sinica Career Development Award 100-CDA-M01 and the National Science Council 98-2112-M01-04-MY3 and 101-2112-M01-03-MY3, and the CUHK C. N. Yang visitor fellowship. I would also like to thank insightful discussions with Patrick S. Doyle, Chia-Fu Chou, Walter Reisner, Robert Austin, Murugappan Muthukumar, Ken Schweizer, and Arsen Grigoryan. Special thanks to Chih-Chen Hsieh for providing the data of DNA persistence length as a function of the ionic strength.

[1]C.-C. Hsieh, A. Balducci, and P. S. Doyle, Macromolecules **40**, 5196 (2007).
[2]J. O. Tegenfeldt, C. Prinz, H. Cao, S. Chou, W. W. Reisner, R. Riehn, Y. M. Wang, E. C. Cox, J. C. Sturm, P. Silberzan, and R. H. Austin, Proc. Natl. Acad. Sci. USA **101**, 10979 (2004).
[3]Y.-L. Chen, M. D. Graham, J. J. de Pablo, G. C. Randall, M. Gupta, and P. S. Doyle, Phys. Rev. E **70**, 060901(R) (2004).
[4]E. A. Strychalski, S. L. Levy, and H. G. Craighead, Macromolecules **41**(20), 7716–7721 (2008).
[5]W. Reisner, K. J. Morton, R. Riehn, Y. M. Wang, Z. Yu, M. Rosen, J. C. Sturm, S. Y. Chou, E. Frey, and R. H. Austin, Phys. Rev. Lett. **94**, 196101 (2005).
[6]P. K. Lin, K. H. Lin, C. C. Fu, K. C. Lee, P. K. Wei, W. W. Pai, P. H. Tsao, Y. L. Chen, and W. S. Fann, Macromolecules **42**(5), 1770–1774 (2009).
[7]P.-K. Lin, J.-F. Chang, C.-H. Wei, P. H. Tsao, W. S. Fann, and Y.-L. Chen, Phys. Rev. E **84**, 031917 (2011).
[8]P.-K. Lin, C.-C. Fu, Y.-L. Chen, Y.-R. Chen, P.-K. Wei, C. H. Kuan, and W. S. Fann, Phys. Rev. E **76**, 011806 (2007).
[9]F. Persson, P. Utko, W. Reisner, N. B. Larsen, and A. Kristensen, Nano Lett. **9**(4), 1382 (2009).
[10]F. Persson, F. Westerlund, J. O. Tegeneldt, and A. Kristensen, Small **5**, 190 (2009).
[11]R. H. Austin, J. O. Tegeneldt, H. Cao, S. Y. Chou, and E. C. Cox, IEEE Trans. Nanotechnol. **1**(1), 12 (2002).
[12]B. Maier and J. O. Rädler, Phys. Rev. Lett. **82**(9), 1911 (1999).
[13]P. Cifra, Z. Benkova, and T. Bleha, Faraday Discuss. **139**, 377–392 (2008).
[14]P. Cifra and T. Bleha, Eur. Phys. J. E **32**(3), 273–279 (2010).
[15]C. W. Hsu and Y. L. Chen, J. Chem. Phys. **133**, 034906 (2010).
[16]J. Tang, D. W. Trahan, and P. S. Doyle, Macromolecules **43**(6), 3081–3089 (2010).
[17]Y. Wang, D. R. Tree, and K. D. Dorfman, Macromolecules **44**, 6594 (2011).
[18]E. A. Strychalski, J. Geist, M. Gaitan, L. E. Locasio, and S. M. Stavis, Macromolecules **45**, 1602 (2012).
[19]T. Odijk, Macromolecules **16**, 1340 (1983).
[20]T. Burkhardt, J. Phys. A: Math. Gen. **28**, L629 (1995).
[21]J. Z. Y. Chen and D. E. Sullivan, Macromolecules **39**, 7769 (2006).
[22]P. Cifra, Z. Benkova, and T. Bleha, Phys. Chem. Chem. Phys. **12**(31), 8934–8943 (2010).
[23]D. R. Tree, Y. Wang, and K. D. Dorfman, Phys. Rev. Lett. **110**, 208103 (2013).
[24]C. -C Hsieh, A. Balducci, and P. S. Doyle, Nano Lett. **8**, 1683 (2008).
[25]D. Stigter, Biopolymers **16**, 1435 (1977).
[26]F. Brochard and P. G. de Gennes, J. Chem. Phys. **67**, 52 (1977).
[27]P. G. deGennes, *Scaling Concepts in Polymer Physics* (Cornell University Press, Ithaca, 1979).
[28]P. J. Flory, *Principals of Polymer Chemistry* (Cornell University Press, Ithaca, NY, 1953).
[29]T. Burkhardt, J. Phys. A: Math. Gen. **30**, L167 (1997).
[30]T. W. Burkhardt, Y. Yang, and G. Gompper, Phys. Rev. E **82**, 041801 (2010).
[31]M. Doi and S. F. Edwards, *Theory of Polymer Dynamics* (Oxford Press, Oxford, 1986).
[32]P. Ahlrichs and B. Dünweg, Int. J. Mod. Phys. C **9**, 1429 (1998).
[33]B. Dünweg and A. J. C. Ladd, Adv. Poly. Sci. **221**, 89 (2008).
[34]G. A. Hegde, J. Chang, Y. Chen, and R. Khare, J. Chem. Phys. **135**(18), 184901-7 (2011).
[35]Y. L. Chen, H. Ma, M. Graham, and J. de Pablo, Macromolecules **40**(16), 5978–5984 (2007).
[36]T. Sakaue, K. Yoshikawa, S. H. Yoshimura, and K. Takeyasu, Phys. Rev. Lett. **87**(7), 078105 (2001).
[37]Y.-L. Chen, P. K. Lin, and C. F. Chou, Macromolecules **43**, 10204 (2010).
[38]R. M. Jendrejack, D. C. Schwartz, M. D. Graham, and J. J. de Pablo, J. Chem. Phys. **119**(2), 1165 (2003).
[39]D. J. Quinn, I. Pivkin, S. Y. Wong, K. H. Chiam, M. Dao, G. E. Karniadakis, and S. Suresh, Ann. Biomed. Eng. **39**(3), 1041–1050 (2011).
[40]T. Odijk, Phys. Rev. E **77**, 060901 (R) (2008).
[41]P. Cifra, Z. Benkova, and T. Bleha, J. Phys. Chem. B **113**(7), 1843–1851 (2009).
[42]Y. Kim, K. S. Kim, K. L. Kounovsky, R. Chang, G. Y. Jung, J. J. dePablo, K. Jo, and D. C. Schwartz, Lab Chip **11**, 1721 (2011).
[43]C. Zhang, F. Zhang, J. A. van Kan, and J. R. C. van der Maarel, J. Chem. Phys. **128**, 225109 (2008).
[44]P. Rouse, J. Chem. Phys. **21**(7), 1272 (1953).
[45]C. Bustamante, Z. Bryant, and S. B. Smith, Nature **421**, 423 (2003).
[46]T. T. Perkins, S. R. Quake, D. E. Smith, and S. Chu, Science **264**, 822 (1994).
[47]D. R. Tree, Y. Wang, and K. D. Dorfman, Biomicrofluidics **7**, 054118 (2013).